Interaction of Charged Surfaces with Grafted Polyelectrolytes: A Poisson–Boltzmann and Monte Carlo Study

S. J. Miklavic, C. E. Woodward, Bo Jönsson,* and T. Åkesson

Physical Chemistry 2, Chemical Center, Box 124, 221 00 Lund, Sweden

Received December 19, 1989; Revised Manuscript Received March 9, 1990

ABSTRACT: We present a Monte Carlo and mean-field study of two charged surfaces with grafted polyelectrolytes, examining the dependence on system parameters of the osmotic pressure as well as intrinsic equilibrium properties of the polyelectrolytes. The polyelectrolyte molecules are modeled as charged monomers connected via suitable bond potentials. The monotonic repulsion between charged surfaces in a simple electrolyte solution, expected from traditional double-layer theory, is not realized in this system. Indeed, we find the force attractive over a wide range of parameter values, with a significant magnitude compared to that of either ordinary double layer or van der Waals forces. The attraction is mainly due to an entropically driven bridging across the gap between the surfaces by the chains, while the attraction due to ion–ion correlation seems to be of minor significance in this system. The mean-field approximation provides a quantitatively correct description of the system, and, most importantly, it responds correctly to changes in parameter space.

Introduction

Polyelectrolyte systems have remained one of the most interesting and challenging areas of colloid science. Leading up to the mid-60s the work of Kuhn and Katchalsky[1-3] and others (see, e.g., Rice and Nagasawa[4]) featured prominently. These have provided the basis of our understanding of macroions in general, though at times having limited application to flexible polyelectrolytes by either placing too great an emphasis on rigid macroions or by suffering from too severe approximations. Then followed a decade or so when theoretical progress lagged considerably behind experimental impetus. In the 1970s further semiquantitative understanding of flexible polyelectrolyte systems was achieved through the efforts of Oosawa,[5] with phenomenological arguments, Odijk[6] and Skolnick and Fixman,[7] working on models of stiff "wormlike" chains, and de Gennes and co-workers,[8] using scaling concepts. More recently quantitative efforts in the form of exact, equilibrium statistical mechanical simulations[9-12] have been made on systems involving isolated polyions in the presence of added salt.

Our own interest centers around forces between macroparticles (often charged), mediated by solvent and other dissolved species. Understanding the nature of these forces is of vital importance to many industrial as well as biological processes.

In the past, computer simulations have illuminated the mechanisms driving the forces between surfaces, as mediated by simple "atomic" particles. In Coulombic systems, for instance, charge correlations have been shown to be important under certain circumstances[13,14] yet are totally neglected in the classical DLVO treatment of colloid interaction, which is based on the mean-field Poisson–Boltzmann theory. Simulations also provide a useful and, at times preferable, alternative to actual experiments when assessing approximate theories.

Recently we reported on Monte Carlo simulations of two charged surfaces with a solution of intervening polyelectrolyte counterions[15] (henceforth referred to as I), calculating the osmotic pressure of the system. One of the most significant findings was that the force was qualitatively different from that expected from DLVO theory. Indeed, we found separations where the pressure was extremely attractive ($P_{osm}/RT \approx -3$ M), which is in contrast to the repulsive force expected in the case of simple *mono*valent counterions.[16] A major source of the attraction is the bridging of the gap between the surfaces by the chains. These bridges literally pull the halves of the system together. This should be distinguished from the attraction found in the case of interacting electrical double layers with divalent (or multivalent) counterions.[14] The latter is mainly an effect of charge fluctuations across the halves and so cannot be predicted by the Poisson–Boltzmann (PB) approximation, which neglects such correlations. On the other hand, a suitably generalized mean-field theory, the Polyelectrolyte Poisson–Boltzmann (PPB) theory, is able to predict an attraction in the polyelectrolyte system, even though electrostatic correlations are still absent.

In this report, we consider the case of polyelectrolyte counterions between charged surfaces, assuming the absence of any simple electrolyte species. The difference between this work and our investigation in I is that the polyelectrolyte molecules are now terminally grafted to the walls with a suitable bonding potential (Figure 1). The force between the charged surfaces is studied for systematic variations of the macroscopic surface charge and the strength of the harmonic potential connecting monomers. A direct comparison of the force profiles for free and grafted chains is made to see whether this additional constraint results in any modification to the force between the surfaces. We also present a new expression for the force between surfaces in polyelectrolyte systems. In this expression the contributions due to bridging and ionic correlations are clearly separable, and thus we are able to quantitatively assess their relative importance. As well as the forces, we also consider the configurational properties of the polyelectrolyte chains. In particular, we present average monomer–monomer and end–end separations.

A direct comparison is made between the simulation results and the PPB theory. By virtue of its relative ease and speed in computing system properties, the latter can also be readily used to explore those regions of parameter space that could prove difficult or time consuming for simulations. For instance, we use here the PPB theory to examine the effect of other types of polyelectrolyte bond functions: a harmonic potential with a nonzero equilibrium bond length and that corresponding to a freely jointed

* To whom correspondence should be addressed.

0024-9297/90/2223-4149$02.50/0

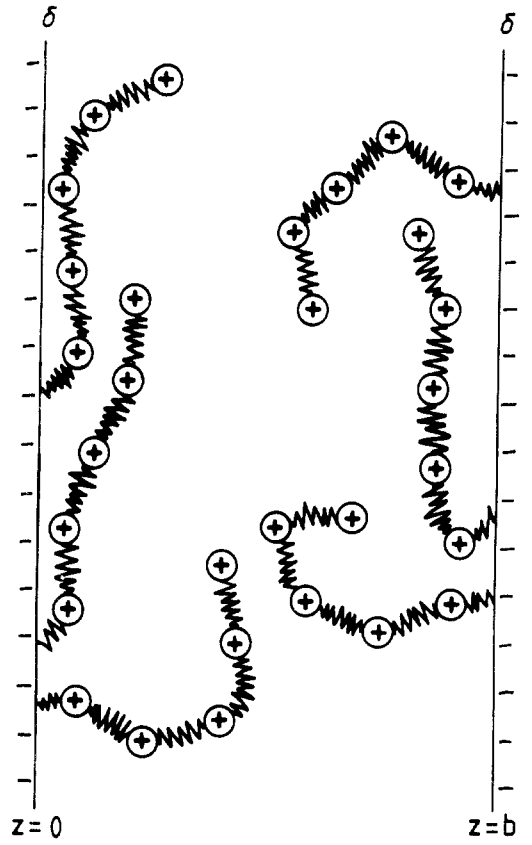

Figure 1. Schematic picture of the system under study. Two charged surfaces with connected counterions, each grafted at one end to one of the surfaces. As drawn the number of charges per chain, n, is 5. The surfaces are separated in a continuum with a dielectric constant, ϵ_r, by a distance b.

chain of fixed bond length.

To obviate any initial criticism of the simplistic model chosen here, we make the following remarks. The counterion-only case not only proves to be the simplest one to study, with the least number of free parameters, but one where the essential physics can readily be extracted. Additional components may introduce competing effects, which, unless they are entered strategically, confuse the interpretation. This has already been borne out in studies involving simple point ions between surfaces and is no less applicable here.

Model System

The model is shown schematically in Figure 1. The z direction is defined to be perpendicular to the parallel walls, one wall being placed at $z = 0$ in the x–y plane and the other at $z = b$. All chains are grafted to either one of the two identical, opposing surfaces, and all monomers have unit positive charge, e. We let n denote the number of charged groups per chain, the same for all chains. No extra short-ranged repulsion between monomers is included; indeed, the direct ion–ion repulsion prevents monomers from approaching too close to each other. The monomers are therefore treated consistently as point particles in both the mean-field calculations and the Monte Carlo simulations. A dielectric continuum of constant relative permittivity, ϵ_r, is used to model the solvent, and the surfaces are treated as hard walls with a uniform negative surface charge of magnitude σ. These each possess an equal number of chains at a grafting density, such that the total polyelectrolyte charge exactly balances the surface charge.

In I, the underlying bond potential, u_b, acting between consecutive charged groups had the form of a simple harmonic potential

$$u_b(r) = Kr^2 \tag{1}$$

where r denotes the separation of nearest-neighbor (NN) charge pairs and K is the force constant.

In reality, to each "monomeric" unit of a polyelectrolyte, one generally associates a charged group and a number of neutral atoms or molecules that maintain the connected structure of the macromolecule. In our work all information concerning these latter atoms is contained in the force constant, K, which is to be interpreted as a result of a preaveraging over all their possible positions and is thus an implicit measure of the persistence length of the underlying chain. Equation 1 is, however, a somewhat simplistic choice for the mechanism giving the connectivity of chains but has the virtue of containing only one parameter. In this work we shall also consider two other, more appropriate, forms of bond potentials: a harmonic potential with a nonzero center of oscillation, a, and a rigid bond distribution, i.e.

$$u_b(r) = K(r - a)^2 \tag{2a}$$

and

$$\exp[-\beta u_b(r)] = \delta(r^2 - a^2) \tag{2b}$$

$\beta = 1/k_BT$, where k_B is Boltzmann's constant and T is the absolute temperature. The latter distribution confines a monomer to the surface of a sphere of radius a about its nearest chain neighbor. Clearly in the limit of $K \to \infty$, eq 2a gives the distribution in eq 2b. These potentials imply a persistence length of the chain equal to the length per unit charge. Apart from connecting monomers, these functional forms, eqs 1 and 2, are also used to enact the grafting to the surfaces. The total potential between NN monomer pairs in a given chain is then

$$u(r) = u_b(r) + e^2/4\pi\epsilon_0\epsilon_r r \tag{3}$$

With $u_b(r)$ given by eq 1, the variable, r_{min}, defined as

$$r_{min} = (e^2/8\pi\epsilon_0\epsilon_r K)^{1/3} \tag{4}$$

being the separation at which $u(r)$ is minimum, is used, rather than K.

Monte Carlo Simulations

In the MC calculation all Coulombic interactions between pairs of molecules contained within the simulation "box" are evaluated. In addition, each particle interacts with two sources of applied field. One is that due to the charge on the surfaces (within the area of the simulation box); the other is a long-range correction. This latter is an externally applied field due to all sources of charge in the box exterior; a nonuniform average distribution of the outer counterions plus the remainder of the surface charge generates a mean field that acts on those ions within the box. The external field is updated with each new simulation run, taking the current concentration profile within the box as the source of the externally applied field in the next iteration. Self-consistency is normally achieved within two or three iterations.

For the following, we consider 240 particles contained within the box whose size is determined from the condition of electroneutrality. This number corresponds to 120 charged monomers, or 12 chains, on each surface, as we fix $n = 10$. Equilibration runs of greater than 50 000 moves per particle were performed prior to all production runs, which in turn were of the order 120–180 000 moves per particle. The particle displacement parameter varied from

3 to 10 Å in order to obtain an acceptance rate of approximately 50% as is customary in standard Metropolis MC algorithms.[17] All calculations were conducted at a temperature T = 298 K and with a dielectric constant of the solvent, ϵ_r, of 78.3.

Polyelectrolyte Poisson–Boltzmann (PPB) Theory

There is an enormous amount of testimony in the literature to the validity of the PB approximation to electrical double layers and of its limiations.[13,14,16,18,19] Given that it is quite accurate in its force predictions for the case of monovalent counterions (normally less than a factor of 2 in error[16]) yet fails qualitatively for divalent counterions, it is surprising and encouraging that the results in I indicate a qualitatively consistent behavior for the case of flexible chains of counterions (compared with the MC).

The PPB approximation combines the configurational statistical mechanics of polymers and the mean-field theory of electrical double layers. The approximation is based on the assumption that all charge interactions, except nearest-neighbor monomers, are suppressed into an average electrostatic potential, $\Psi(z)$. It has been shown in I that by minimizing an appropriate free energy functional the density distribution of polyelectrolyte molecules, grafted to the wall at $z = b$, say, with monomers in the configuration $\xi = \{\mathbf{r}_0; \mathbf{r}_1, \ldots \mathbf{r}_n\}$, takes the form

$$\rho_p(\xi) = \mathcal{N}\delta(z_0-b)\, w_g(|\mathbf{r}_1-\mathbf{r}_0|)\, e^{-\beta e\Psi(z_1)} w(|\mathbf{r}_2-\mathbf{r}_1|)\, e^{-\beta e\Psi(z_2)} \ldots e^{-\beta e\Psi(z_2)} w(|\mathbf{r}_n-\mathbf{r}_{n-1}|) \quad (5)$$

where $\mathbf{r}_0$ is the position of the surface grafting point. A similar expression holds for those chains grafted to the wall at $z = 0$. In the present symmetry, $\Psi(z)$, is a one-dimensional mean electrostatic potential. The function $w(r) = \exp[-\beta u(r)]$ with u given by eq 3, and the grafting function $w_g(r) = \exp[-\beta u_b(r)]$. $\mathcal{N}$ is a normalization constant, such that $\rho_p(\xi)$ is to be interpreted as the number density of polyions with the configuration ξ.

As has been discussed in I, the inclusion of the nearest-neighbor (NN) Coulombic repulsions in the bond distribution function, w, is in recognition of the fact that the strong electrostatic correlations along local sections of the polyelectrolyte chains would be inadequately described by the mean field. For strong polyelectrolytes, where monomers separated by more than one bond are constrained to be close to one another, one would like to include interactions beyond NN. Unfortunately, this would lead to a set of equations that is very difficult to solve and we restrict ourselves to the nearest-neighbor case. The implications of this, and the neglect of electrostatic correlations in general, will be discussed in the comparison between the PPB and MC results.

The electrostatic potential, Ψ, satisifies the Poisson equation

$$\frac{d^2}{dz^2}\Psi(z) = -\frac{4\pi}{\epsilon}\rho_m(z) \quad (6)$$

together with the appropriate boundary conditions on the electric field. ρ_m is the local average monomer density, which has the form

$$\rho_m(z) = \int d\xi \sum_{i=1}^{n} \delta(z\mathbf{k}-\mathbf{r}_i)\, \rho_p(\xi) \quad (7)$$

where $\mathbf{k}$ is a unit vector normal to the surface. Equations 5–7 provide a self-consistent set of equations, which can be solved iteratively. As Ψ is only a function of z, the lateral integrations in eq 7 only involve the functions w. It is thus useful to define the laterally integrated bond function, $v(z-z')$, given by

$$v(z-z') = 2\pi \int_0^\infty \rho\, d\rho\, w(z-z',\rho) \quad (8)$$

where

$$|\mathbf{r}-\mathbf{r}'| = \sqrt{(z-z')^2 + |\rho-\rho'|^2} \quad (9)$$

In the numerics, the upper limit of this integral is chosen to be large and finite. A correction term is then included, assuming that for the remainder of the integration range the contribution to w from the Coulombic potential is negligible. The accuracy of our calculation has been tested by both increasing the value of cutoff and the number of grid points in the numerically integrated range. This lateral averaging needs only to be performed once for each set of parameters (e.g., σ, b, r_{min}), as it is outside the self-consistent iteration loop. The final z integrations are evaluated by discretizing the range $(0,b]$ and treating the values of v as components of a matrix (with indices related to the discretized z,z'). Straightforward matrix multiplication then replaces the continuous integration. Thus the solution algorithm is easily vectorized for optimal computational speed.

Osmotic Pressure

In I we used the contact theorem

$$p_{osm} = k_B T \rho_m(b) - \sigma^2/2\epsilon_0\epsilon_r \quad (10)$$

to give the pressure, p_{osm}, between two charged surfaces with intervening polyelectrolyte counterions. This expression relates the pressure to the surface charge density, σ, and the *monomer* density at the surface at b, $\rho_m(b)$. It has the same form as in the case of simple point counterions.[16] Also as is the case for simple ions, this expression is valid in the PPB theory. We have shown recently that, for grafted chains, eq 10 must be modified[20] to

$$p_{osm} = k_B T \rho_m(b) - \sigma^2/2\epsilon_0\epsilon_r - \langle \partial u_{grf}/\partial b \rangle \quad (11)$$

u_{grf} is the interaction per unit area between the wall at b and its grafted monomers and $\langle\ \rangle$ indicates the ensemble average. Equation 11 is an exact expression, which again applies to the approximate PPB theory. The explicit form of the grafting term varies depending on the type of bond potential assumed. For example, the distribution in eq 2b leads to[20]

$$\langle \partial u_{grf}/\partial b \rangle = k_B T \rho_1(a) \quad (12)$$

where $\rho_1(a)$ is the average number density of the *first* monomers, i.e., those that are directly grafted to a particular surface, evaluated a distance a from that surface.

The contact formulas, eqs 10 and 11, can be thought of as the result of an infinitesimal increase in the wall separation, via a two-step process. In the first step the wall at b is pulled away from the fluid, creating a small gap. This step requires a certain force per unit area, given by the field term, and, in the case of eq 11, an additional stretching of the grafting bonds. The relaxation of the fluid to fill the created gap regains some of the energy loss in the initial step, the work per unit volume being given by the local monomer density. An alternative formulation of the osmotic pressure can be obtained by increasing the wall separation, by firstly separating the fluid halves on either side of the midplane. By a reasoning similar to that

given above, the osmotic pressure is then given by

$$p_{osm} = k_B T \rho_m(b/2) + p_{corr} + p_{brg} \quad (13)$$

which is valid for both grafted and free chains. $\rho_m(b/2)$ is the monomer density at the midplane and $p_{corr} + p_{brg}$ is the average force per unit area necessary to initially separate the fluid halves. The first contribution is due to correlated ion–ion fluctuations on either side of the midplane, and the second is due to the stretching of those polyelectrolyte bonds that cross the midplane. One can show that

$$p_{corr} = \frac{1}{A}\int_{z_1<b/2} d\mathbf{r}_1 \int_{z_2>b/2} d\mathbf{r}_2\, \Delta\rho^{(2)}(\mathbf{r}_1,\mathbf{r}_2) \times \frac{\partial|\mathbf{r}_1-\mathbf{r}_2|^{-1}}{\partial z_1} e^2/4\pi\epsilon_0\epsilon_r \quad (14)$$

We let A formally denote the walls' areas, where it is understood that we take the limit $A \to \infty$. The two-particle density correlation function is defined by

$$\Delta\rho^{(2)}(\mathbf{r}_1,\mathbf{r}_2) = \sum_{k,k'} \sum_{i,j=1}^{n}{}' \langle \delta(\mathbf{r}_1-\mathbf{r}_i^k)\,(\mathbf{r}_2-\mathbf{r}_i^{k'})\rangle - \rho_m(\mathbf{r}_1)\,\rho_m(\mathbf{r}_2) \quad (15)$$

with

$$\rho_m(\mathbf{r}_1) = \sum_k \sum_{i=1}^{n} \langle \delta(\mathbf{r}_1-\mathbf{r}_i^k)\rangle \quad (16)$$

The notation is such that the monomers on a given polyelectrolyte chain, k, are sequentially labeled with the subscript i such that $i = 1$ corresponds to the monomer that is directly attached to a surface. The prime on the summation in eq 16 means that $i \neq j$ for $k = k'$.

We also have

$$p_{brg} = \frac{1}{A}\int_{z_1<b/2} d\mathbf{r}_1 \int_{z_2>b/2} d\mathbf{r}_2\, n^{(2)}(\mathbf{r}_1,\mathbf{r}_2)\frac{\partial u_b(|\mathbf{r}_1-\mathbf{r}_2|)}{\partial z_1} + \frac{2}{A}\int_{z_1<b/2} d\mathbf{r}_1 \int d\mathbf{r}_0\, m^{(2)}(\mathbf{r}_1,\mathbf{r}_0)\frac{\partial u_b(|\mathbf{r}_1-\mathbf{r}_0|)}{\partial z_1} \quad (17)$$

where $n^{(2)}(\mathbf{r}_1,\mathbf{r}_2)$ is the density distribution for all nearest-neighbor monomer pairs, i.e.

$$n^{(2)}(\mathbf{r}_1,\mathbf{r}_2) = \sum_k \sum_{i=1}^{n-1} \langle \delta(\mathbf{r}_1-\mathbf{r}_i^k)\,\delta(\mathbf{r}_2-\mathbf{r}_{i+1}^k)\rangle \quad (18)$$

Thus the first term in eq 17 describes the stretching of monomer–monomer bonds across the midplane. The second term accounts for the monomer–surface bonds that cross the midplane. The actual point of attachment of the first monomer of the kth chain to the surface at b is denoted as $\mathbf{r}_0^k$, and we define

$$m^{(2)}(\mathbf{r}_1,\mathbf{r}_0) = \sum_k{}' \langle \delta(\mathbf{r}_1-\mathbf{r}_1^k)\,\delta(\mathbf{r}_0-\mathbf{r}_0^k)\rangle \quad (19)$$

The prime on the summation means we sum only over chains attached to the surface at b.

Apart from p_{brg}, eq 13 is exactly the same as that derived for the simple ion case.[16] As p_{brg} is due to chains that connect the half regions with at least one crossing bond (*bridging* chains), we call it the "bridging pressure". Note that our definition of bridging chains is more general than that used by other authors.[21]

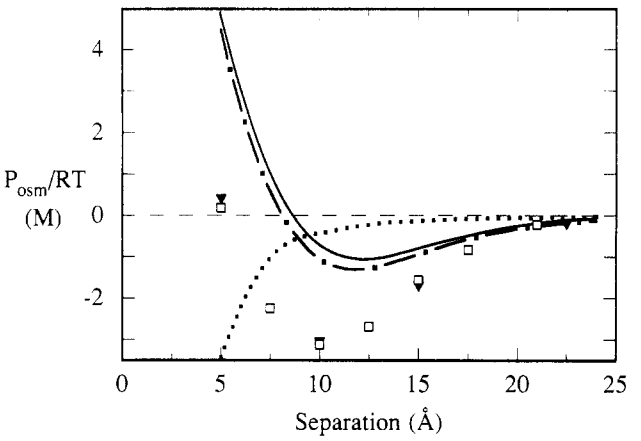

Figure 2. Osmotic pressure as a function of separation. The symbols represent MC results: filled nablas for the case of "free" polyelectrolytes and open squares for the case of "grafted" polyelectrolytes. The continuous curves are the PPB results for the same systems (solid and broken line as calculated with eqs 10 and 11, respectively). $\sigma = 0.224$ C/m^2 and $r_{min} = 5$ Å. In this figure and all figures below the number of charged units on each chain is 10. The dotted curve shows a van der Waals (attractive) pressure, $P_{vdw} = -A/6\pi b^3$, with a Hamaker constant of $A = 2.0 \times 10^{-20}$ J.

An analysis of the PPB theory gives the following expression for the osmotic pressure:

$$p_{osm} = k_B T \rho_m(b/2) + p_{corr}^{PPB} + p_{brg} \quad (20)$$

One should compare this with the exact result (eq 13). The expression for the bridging pressure is exactly the same as eq 17, except that the PPB approximations replace the exact density functions of eqs 18 and 19. The PPB expression also contains a contribution from electrostatic correlations across the midplane, given explicity by

$$p_{corr}^{PPB} = \frac{1}{A}\int_{z_1<b/2} d\mathbf{r}_1 \int_{z_2>b/2} d\mathbf{r}_2\, n^{(2)}(\mathbf{r}_1,\mathbf{r}_2) \times \frac{\partial|\mathbf{r}_1-\mathbf{r}_2|^{-1}}{\partial z_1} e^2/4\pi\epsilon_0\epsilon_r \quad (21)$$

This term arises due to the inclusion of NN Coulombic repulsions in the PPB description of the chain configurations (eq 5). As it is *only* NN pairs that have a direct electrostatic interaction, the distribution of nearest-neighbor pairs, $n^{(2)}$, replaces the *full* pair density distribution function, $\Delta\rho^{(2)}$, in eq 14. It is clear that this term gives a repulsive contribution to the osmotic pressure, whereas one expects the full p_{corr} (eq 14) to be attractive. We will see later that better agreement with the simulations is obtained by neglecting this contribution to the total PPB pressure.

Results and Discussion

(i) Osmotic Pressure. In Figure 2 we compare the pressure versus separation curves for the two model systems of free and grafted chains, calculated by using MC simulation and the PPB approximation. The MC values were most easily obtained by using the contact expression (eqs 10 and 11). In the PPB calculations, pressures obtained by using the contact expression or eq 20 generally agreed to within a few percent, which indicates our solutions were numerically accurate. The surface charge density is 0.224 C/m^2, and a harmonic bonding potential, as given by eq 1, is used with $r_{min} = 5$ Å. This gave an average monomer–monomer separation of about 7.5–8 Å, depending on the wall separation. No significant difference in the pressures appears to exist between the two model

systems. To within simulation error, the MC predicts virtually the same forces; likewise, the PPB results suggest little difference. Also included in Figure 2 is a van der Waals attractive pressure, $p_{vdw} = -A/6\pi b^3$, valid for two planar interfaces, where A is the Hamaker constant. This is shown for purposes of comparison and has not been included in the calculation of the forces discussed here. A Hamaker strength of 2.0×10^{-20} J was chosen, corresponding to the force between mica surfaces across water. It is shown to be completely overwhelmed by the polyelectrolyte-mediated forces in both magnitude and range. This is certainly of significance in biological processes as well as for the practical purpose of colloidal flocculation.

A likely reason for the similarity in forces for the two model systems is that, at the separations considered here (certainly at around the force minimum and inward), a substantial number of the monomers are actually quite close to the walls. Thus it does not matter so much if the chains are pinned to a surface or not. One would expect relative differences between the force curves to show up at larger separations, but the decreasing numerical accuracy of both the MC and PPB would make their detection difficult. In any case, the small magnitude of the force at these separations would make the discrepancies less interesting. The agreement shown in Figure 2 is expected to persist under most conditions of surface charge and bond strengths, and conclusions to be given in this report, although based on the chains being in the grafted state, are also pertinent to a system with free polyelectrolytes between the walls.

The PPB theory, though predicting a significant attraction when compared with the van der Waals pressure, significantly underestimates the depth of the force minimum in Figure 2. Furthermore, the position of the minimum is shifted slightly outward when compared with the Monte Carlo results. Some understanding of this discrepancy can be obtained by decomposing the MC pressure into the bridging and electrostatic correlation contributions as suggested by eq 13. These were obtained from the MC by calculating the midplane monomer concentration and the bridging contribution, p_{brg}, explicitly. The electrostatic correlation contribution, p_{corr}, was obtained from the total pressure, evaluated by using the contact formula. The various contributions are plotted in Figure 3. We show also the PPB results for the total osmotic pressure *upon removing the repulsive nearest-neighbor Coulombic term* of eq 20 and the PPB prediction for p_{brg}. The Monte Carlo results show that, at around the force minimum and outward, the electrostatic correlation pressure, p_{corr}, is small in magnitude relative to the bridging pressure. This suggests that the repulsive NN electrostatic correlations, p_{corr}^{PPB}, are largely cancelled by the rest of the electrostatic correlations, at these separations, and that a better result would be had by neglecting this term. The total PPB pressure then becomes just the sum of the midplane monomer concentration and the bridging contribution. The better quantitative agreement with the simulated pressure curves, in both the depth and position of the minimum, obtained with this "recipe" is evident. This is due to the remarkable agreement between the PPB and MC predictions for the bridging pressure, at all separations. At small separations the electrostatic correlation contribution becomes larger, as it should, and at 5 Å it has almost the same magnitude as the bridging term. It is here that the difference between the MC and PPB total pressures is largest; indeed, it appears that the correlation term accounts for almost all

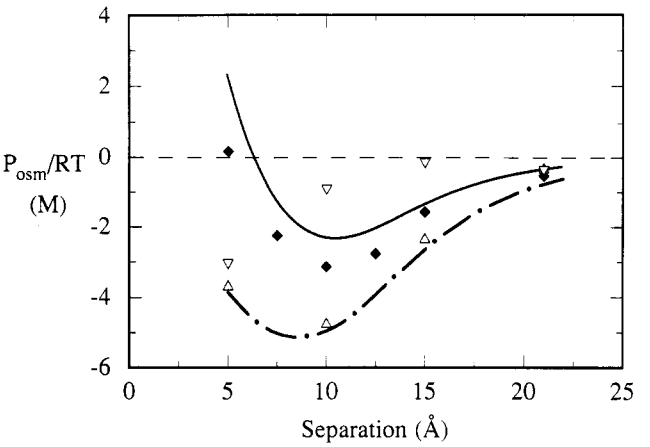

Figure 3. Pressure contributions vs separation. These results correspond to the parameter set shown in the previous figure. They are calculated according to the terms appearing in eq 20. Open nablas refer to the correlation contribution, p_{corr}; open triangles and dot-dashed curve represent the bridging contribution, p_{brg}, as calculated with both the MC and the PPB methods; finally the filled diamonds and solid line show the total pressure from the two methods.

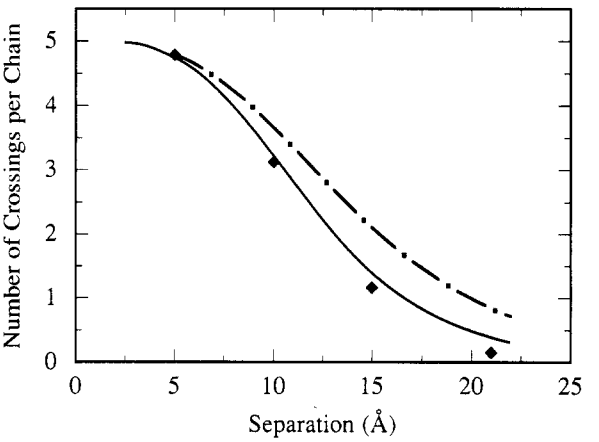

Figure 4. Total number of chains crossing the midplane vs separation calculated with $r_{min} = 5$ Å. Filled diamonds and solid curve show the MC and PPB results for $\sigma = 0.224$ C/m², while the dot-dashed curve shows the PPB predictions for the surface charge of $\sigma = 0.1$ C/m².

the discrepancy between MC and PPB results for the total force. In the PPB calculations below, we will only quote results pertaining to the exclusion of the p_{corr}^{PPB} term.

The parameters chosen here correspond to relatively high charge densities on both the surfaces and the polyelectrolytes. Thus, on past experience,[14,16] one would anticipate that the electrostatic correlation contribution to the pressure here would be about as large as could be expected for any experimentally realizable scenario. Nevertheless, the attraction depicted in Figures 2 and 3 can be attributed mainly to the influence of bridging chains. Chains bridge in order to maximize their configurational entropy; this is done at a cost in energy. The number of bridges formed is thus a compromise between these two effects. Figure 4 depicts the average number of bonds per chain that cross the midplane, as a function of the separation. As expected their number falls off at larger separation. As the separation decreases the number of bridging bonds saturates, so that in the end about half of the bonds in any chain bridge: a pair of NN monomers is more or less equally likely to sit on the same surface as on opposing surfaces. The bridging pressure curve (Figure 3) can be thought of as a product of the number of bridges and the average force or "tension" per bridging bond; one would

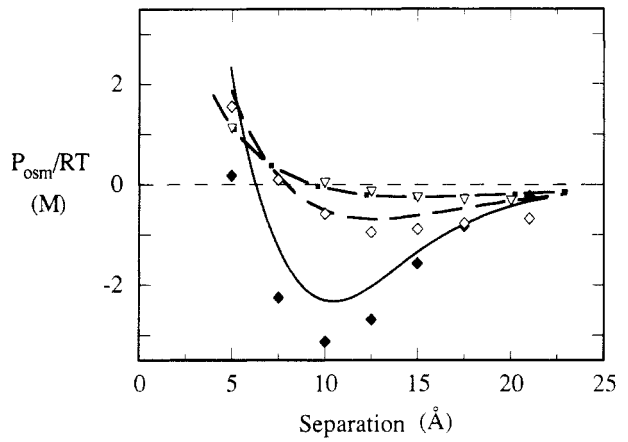

Figure 5. Total osmotic pressure vs separation for different values of surface charge density. MC results are again shown as symbols and PPB as continuous curves: $\sigma = 0.224$ C/m^2, filled diamonds and solid line; $\sigma = 0.1$ C/m^2, open diamonds and dashed line; $\sigma = 0.05$ C/m^2, open nablas and dot-dashed line. r_{min} is again fixed at 5 Å.

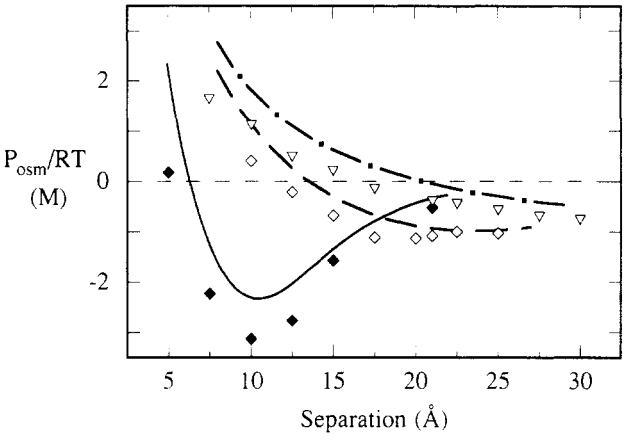

Figure 6. Total osmotic pressure vs separation for different values of r_{min}. Filled diamonds and solid line correspond to r_{min} = 5 Å; open diamonds and dashed line corresponds to r_{min} = 10 Å; open nablas and dot-dashed line correspond to r_{min} = 15 Å. σ = 0.224 C/m^2 throughout.

expect this latter function to increase with separation, giving a maximum in the bridging force curve at a separation of about 10 Å. The PPB theory does extremely well in predicting the number of bridging bonds, implying that correlation effects (both intra- and interchain) appear to play a small role in determining these. For comparison, we show the PPB results at a lower surface charge density of 0.1 C/m^2.

What then is the effect on the osmotic pressure of decreasing the surface charge? In a salt-free system, one is forced to simultaneously reduce the polyelectrolyte concentration. Figure 5 shows that a sizeable decrease in both the MC and PPB pressures ensues as the surface charge density varies from 0.224 to 0.05 C/m^2. The PPB does a reasonably good job in reproducing this behavior. This implies that the major cause is the decrease in the bridging pressure, though electrostatic correlations *between* chains also become less important, at the lower chain density. Analysis of the PPB results shows that, apart from the actual number of bridges decreasing, the falloff with separation of the number of bridges per chain is less rapid, as the surface charge density decreases (see Figure 4). At the same time, one would expect that the average tension in a bridging bond is reduced, due to the smaller electrostatic potential at the walls. The result is that the force minima in Figure 5 become much shallower and are shifted to larger separations with decreasing σ.

In the limit of infinite r_{min} (or zero K), the chains lose their definition, and the interaction pressure reverts back to the case of the ordinary repulsive double-layer force.[16] One interesting question then concerns the behavior of the force curve as this limit is sought. Figure 6 shows the force curves for three values of r_{min}, at a fixed surface charge density of 0.224 C/m^2.

Though the uncertainty in the MC results increases with r_{min}, the position of the force minimum clearly shifts to larger separations with the attraction at this point becoming weaker. Both these observations concur with physical anticipations: as r_{min} increases the average monomer–monomer distance also increases so that bridges can form at larger separations. The average bond tension, however, decreases, and the strength of the bridging pressure diminishes. Weaker polyelectrolytes, that is, polyelectrolytes having a larger r_{min} and thus a smaller linear charge density, thus mediate the greatest attraction at larger wall separations. It should be kept in mind that the attractive forces depicted in Figure 6 are by no means

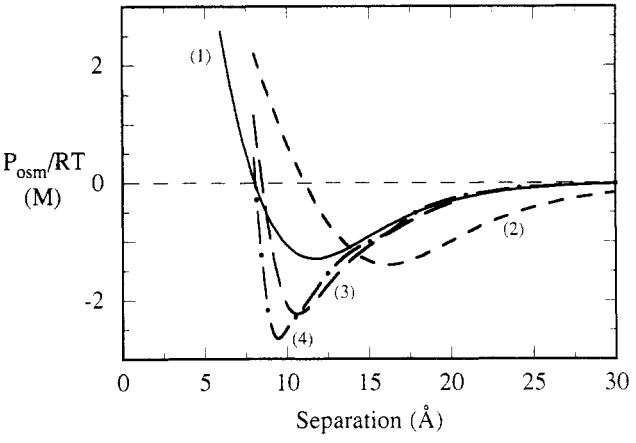

Figure 7. Osmotic pressure vs separation, as calculated with the PPB model for different bond functions. σ = 0.224 C/m^2 throughout. Curve (1) corresponds to the use of the bond function eq 1 with r_{min} = 5 Å. Curve (2) results from using eq 2a with $K = e^2/2\epsilon r_{min}^3$ and r_{min} = 5 Å and a value of a = 7.9 Å. Curve (3) is found under the same conditions as curve (2) except that r_{min} = 2 Å. Curve (4) results from the use of eq 2b again with a = 7.9 Å.

insignificant and are certainly at least 1 order of magnitude larger than the van der Waals force. The PPB theory successfully predicts these changes with r_{min}; the NN contribution to the pressure becomes smaller with increasing r_{min} as should be expected. It is easy to imagine that, in the limiting case of infinite r_{min}, the force minimum tends to infinity, while the bridging force goes to zero. Thus the total force once again becomes monotonically repulsive.

The final item we discuss is the behavior of the interaction curves shown in Figure 7. Here the four profiles represent different bonding potentials, of the type shown in eqs 1 and 2, at the same surface charge density of 0.224 C/m^2. These are all results obtained by using the PPB theory where p_{corr}^{PPB} has *not* been subtracted. Curve 1 represents the pressure using the simple harmonic form (eq 1) with r_{min} = 5 Å. From Figure 8, this gave a rms monomer–monomer separation of about 7.9 Å. This value is also taken for the center of oscillation, a, in eq 2a and for the rigid bond distance in eq 2b. The former case, using a force constant K, corresponding to r_{min} = 5 Å, results in curve 2. The effect is to increase the range of the interaction. The force minimum increases from about 12 to 16 Å, but the strength of the attraction is virtually unchanged. This observation suggests that the range of

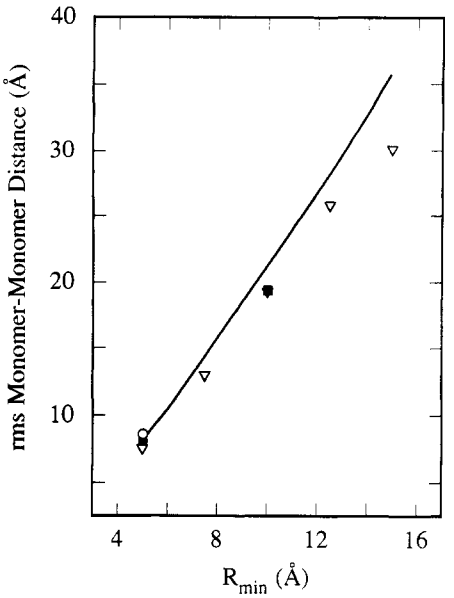

Figure 8. Rms monomer–monomer distances vs r_{min} for different values of the surface charge, at a fixed surface separation of 21 Å. The MC results appear as follows: open nablas, σ = 0.224 C/m²; filled squares, σ = 0.1 C/m²; open circles, σ = 0.05 C/m². The *single* PPB curve represents a surface charge of σ = 0.224 C/m², but the results for the other values of σ are virtually identical and so are not shown.

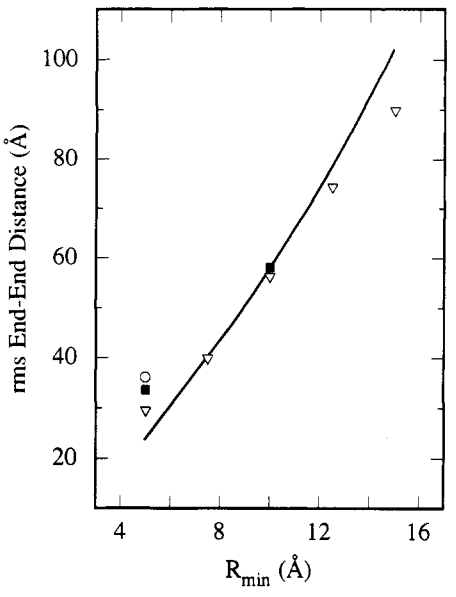

Figure 9. Rms end–end distances vs r_{min}. The results and markings correspond exactly to those of Figure 8.

the attractive bridging contribution can be increased, without reducing its strength significantly, by appropriately decreasing the charge per unit length (increasing a) while maintaining a high tension (K) in the polyelectrolyte molecules. Increasing the force constant by a factor of approximately 64 (corresponding to r_{min} = 2 Å) produces curve 3. The force minimum becomes deeper and shifts in to the center of the bond oscillation, a. The final curve (4) corresponds to the rigid bond distribution (eq 2b) with a = 7.9 Å. With this distribution the force minimum is down at 9.5 Å, and the attraction is still deeper. As anticipated, curve 4 is evidently the limit of curves 2 and 3 as $K \to \infty$ or $r_{min} \to 0$.

(ii) Chain Configurations. From the simulations we calculated two different internal chain lengths as a function of surface separation, b, and charge density, σ. They were the chain-averaged, root-mean-square (rms) monomer–monomer separation, $\langle r_{mm}^2 \rangle^{1/2}$, and the rms end–end separation, $\langle r_{ee}^2 \rangle^{1/2}$, where

$$\langle r_{mm}^2 \rangle^{1/2} = \frac{1}{nN_{total}} \sum_{k=1}^{N_{total}} \sum_{i=0}^{n-1} [\langle |\mathbf{r}_i^k - \mathbf{r}_{i+1}^k|^2 \rangle]^{1/2} \quad (22)$$

and

$$\langle r_{ee}^2 \rangle^{1/2} = \frac{1}{N_{total}} \sum_{k=1}^{N_{total}} [\langle |\mathbf{r}_n^k - \mathbf{r}_0^k|^2 \rangle]^{1/2} \quad (23)$$

N_{total} is the total number of simulated chains. The rms monomer–monomer separation, which we might also call the averaged bond length, gives a measure of the polyelectrolyte strength and (apart from the number of monomers) is the only parameter one has to "fit" to real polyelectrolytes. Figure 8 shows the MC and PPB results for $\langle r_{mm}^2 \rangle^{1/2}$ at several charge densities for varying r_{min}, at a wall separation of 21 Å. Even though the flexible, harmonic potential bond of eq 1 was used, the averaged bond length is fairly insensitive to either the presence of other chains or changes in the external potential. There is a slight increase with wall separation, also predicted by the PPB, which is a consequence of the stretching of bonds as the walls move apart. Indeed, the overall excellent agreement with the PPB theory implies that it is mainly the nearest-neighbor Coulombic interactions that are essential for the determination of the bond length. The PPB does, however, begin to fail at large r_{min}. The most likely reason here is the neglect of correlations to other monomers, which provides an electrostatic screening effect. Although screening is normally associated with an added electrolyte, a finite number of monomers also mutually screens each others electrostatic interactions. The MC averaged bond lengths should then become smaller than the PPB values, as the bond length approaches the "screening length".

Figure 9 shows the rms end–end separation as a function of r_{min}, again at b = 21 Å. The PPB curves for all surface charge densities and separations were almost identical, and only one is shown. At r_{min} = 5 Å, where the the polyelectrolyte has a high charge density, the PPB theory underestimates the MC results. This is due to the neglect of intrachain, electrostatic repulsions, which extend beyond nearest neighbors and tend to favor "stretched" configurations. In the PPB all interactions beyond nearest neighbors have been reduced to a mean potential, $\Psi(z)$. This potential responds only to variations in the average monomer density, while the rms end–end distance is dependent on specific monomer–monomer correlations. The MC results also show a significant decrease in the total rms end–end distances with increasing surface charge density. The effect of electrostatic screening, discussed above, is sufficient to explain this trend. Other things being equal, as the monomer concentration decreases, this screening is reduced. The approximations within the PPB also fail to reproduce this effect. It is symptomatic that the agreement between PPB and MC improves with increasing surface charge density.

For intermediate polyelectrolyte strength (r_{min} = 7–15 Å), the PPB and MC results are quite close. Here the Coulombic correlations appear to be largely screened out beyond the nearest-neighbor distance (about 13–20 Å). For weaker polyelectrolytes, $r_{min} \geq 15$ Å, even nearest-neighbor interactions are screened and the PPB theory overestimates the end–end separation. Thus in PPB solutions for weak polyelectrolytes it would be more appropriate to remove the nearest-neighbor Coulombic repulsion, not only in the force but also in the

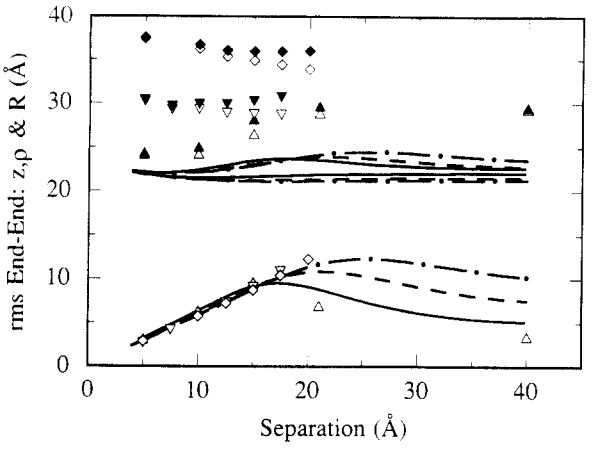

Figure 10. Rms end–end distance and components vs separation for different surfaces charges. The MC and PPB values are represented as follows: open triangles and solid lines for a surface charge of $\sigma = 0.224$ C/m^2; nablas and dashed curves for $\sigma = 0.1$ C/m^2; diamonds and dot-dashed curves for $\sigma = 0.05$ C/m^2. The results shown in the lower half of the figure are the rms z components; the remaining open symbols, and PPB curves in the midst of the figure, are lateral components while the filled symbols and uppermost PPB curves are the total end–end distances. In all cases $r_{min} = 5$ Å.

determination of the polymer density itself (cf. eq 5).

In Figure 10 we hold r_{min} fixed at 5 Å and plot, as a function of b, $\langle r_{ee}^2\rangle^{1/2}$ as well as its "projections" in the z and x–y directions, respectively defined by

$$\frac{1}{N_{total}}\sum_{k=1}^{N_{total}}[\langle(z_n^k - z_0^k)^2\rangle]^{1/2} \qquad (24)$$

and

$$\frac{1}{N_{total}}\sum_{k=1}^{N_{total}}[\langle(x_n^k - x_0^k)^2 + (y_n^k - y_0^k)^2\rangle]^{1/2} \qquad (25)$$

As was indicated in Figure 9 there is a marked decrease in $\langle r_{ee}^2\rangle^{1/2}$ with increasing surface charge density. A survey of the various projections will confirm that most of the reduction comes from the x–y component. Up to about $b = 17$ Å, the z component is rather insensitive to the chain density and appears to be established by the wall separation. In essence the screening effect is "felt" only in the two dimensions parallel to the walls. The PPB predictions for this component confirm the lack of electrostatic correlation in the theory. The MC results also show a weak variation in this component with surface separation.

As the separation increases from 5 to 17 Å, the average z component of the rms end–end separation follows almost linearly, with approximately the same slope (approximately 1.6) for all surface charge densities. These numbers are very well reproduced by the PPB theory, showing that it has captured the essence of the mechanism. The linear behavior and its slope are in fact characteristic of the case where the z positions of the end monomers are largely uncorrelated as the following "mean-field" argument shows. Consider the case of a polyelectrolyte molecule with one end fixed to a wall and the other end uniformly sampling the whole gap, this would approximate the case of a very weak surface charge density. The z component of the rms end–end separation for this molecule is then given by $\sqrt{3}b$. Suppose instead, one now has a high surface charge density so that the free end saw a very attractive potential close to each wall. In that case one could approximately say that it spent half of the time at one wall and the rest of the time at the other, leading to the z component of $\sqrt{2}b$. The situation at intermediate surface charge density is expected to be somewhere in between. On the scale of Figure 10, this leads to a line with a slope somewhere between $\sqrt{3}$ and $\sqrt{2}$.

Beyond about 17 Å we see a marked departure from linear behavior. Now the two end monomers are significantly correlated, the free end being more likely found at the same wall as the grafted end. This is no doubt due to the higher energetic cost of bridging at larger surface separation and at higher surface charge density. The latter effect is confirmed by the PPB calculations at other surface charge densities. One can liken the process to a "snapping" of the polyelectrolyte fluid bridge between the two surfaces. This occurs irrespective of whether the polyelectrolyte chains are grafted to the surfaces or not. Monte Carlo simulations of free polyelectrolyte chains, at the highest charge density and under the same conditions, produce almost identical behavior.

Conclusions

We have presented a study of two charged surfaces bearing polyelectrolyte chains, examining the dependence on system parameters of both the osmotic pressure and configurational properties of these polyelectrolytes.

The mean-field polyelectrolyte Poisson-Boltzmann approximation responds correctly to these changes in parameter space. We found that the osmotic forces predicted by the PPB theory could be brought into better agreement with the MC results if one neglected the contribution due to nearest-neighbor Coulombic repulsions across the midplane. These nearest-neighbor interactions are important for the prediction of the internal chain statistics (the rms bond–bond separation and rms end–end distances) as they represent strong correlations, which cannot be accounted for by a mean field. On the other hand, it appears that their contribution to the pressure, made explicit in eq 20, is more than compensated by the other electrostatic correlations *not* included in the PPB theory. We showed that the PPB theory can do an excellent job in reproducing the purely bridging contribution to the osmotic pressure. The bridging pressure dominates at around the force minimum in the highly coupled system studied in Figure 3, where the electrostatic correlations are about as large as could be expected in real systems. Thus bridging has been firmly established as being the main source of the attractive forces mediated by flexible polyelectrolyte between oppositely charged surfaces. We have shown that this attraction persists and remains significant, even in weakly coupled cases (small σ and large r_{min}). In problems of colloidal flocculation this may be immensely important. Under the right conditions a polyelectrolyte solution appears to be a far more effective flocculent than a simple electrolyte solution.

The results for the internal chain statistics, especially the rms end–end separations, clearly showed the effect of screening due to electrostatic interactions between monomers. The failure of the PPB theory to include this effect is demonstrated in Figures 8–10.

Now that we have laid a firm physical foundation in the understanding of this system, we are able to include effects of other monatomic species (salt and simple counterions) as well as to consider other charge configurations. These future contemplations will go some way to bridge the gap that currently exists between the simple, but fundamental, model used here and the more complicated systems present in experiments.

References and Notes

(1) Kuhn, W.; Kunzle, O.; Katchalsky, A. *J. Phys. Chem.* **1948**, *31*, 1994.
(2) Katchalsky, A.; Kunzle, O.; Kuhn, W. *J. Poly. Sci.* **1950**, *5*, 283.
(3) Katchalsky, A.; Lifson, S. *J. Polym. Sci.* **1956**, *11*, 409.
(4) Rice, S. A.; Nagasawa, M. *Polyelectrolyte Solutions*; Academic Press: New York, 1961, and references therein.
(5) Oosawa, F. *Polyelectrolytes*; Marcel Dekker: New York, 1971.
(6) Odijk, T. *J. Polym. Sci., Polym. Phys. Ed.* **1977**, *15*, 477; *Lect. Notes Phys.* **1982**, *172*, 184.
(7) Skolnick, J.; Fixman, M. *Macromolecules* **1977**, *10*, 944.
(8) de Gennes, P.-G. *Scaling Concepts in Polymer Physics*; Cornell University Press: Ithaca, NY, 1979, and references therein.
(9) Brender, C.; Lax, M.; Windwer, S. *J. Chem. Phys.* **1984**, *80*, 886.
(10) Valleau, J. P. *Chem. Phys.* **1989**, *129*, 163.
(11) Christos, G. A.; Carnie, S. L. *J. Chem. Phys.* **1989**, *91*, 439.
(12) Jönsson, B.; Woodward, C. E., submitted for publication in *J. Phys. Chem.*
(13) Carnie, S. L.; Torrie, G. M. *Adv. Chem. Phys.* **1984**, *56*, 141.
(14) Guldbrand, L.; Jönsson, B.; Wennerström, H.; Linse, P. *J. Chem. Phys.* **1984**, *80*, 2221.
(15) Åkesson, T.; Woodward, C. E.; Jönsson, B. *J. Chem. Phys.* **1989**, *91*, 2461.
(16) Henderson, D.; Blum, L. *J. Chem. Phys.* **1978**, *69*, 5441. Henderson, D.; Blum, L.; Lebowitz, J. L. *J. Electroanal. Chem.* **1979**, *102*, 315. Wennerström, H.; jönsson, B.; Linse, P. *J. Chem. Phys.* **1982**, *76*, 4665.
(17) Metropolis, N. A.; Rosenbluth, A. W.; Rosenbluth, M. N.; Teller, A.; Teller, E. *J. Chem. Phys.* **1953**, *21*, 1087.
(18) Torrie, G. M.; Valleau, J. P. *Chem. Phys. Lett.* **1979**, *65*, 343.
(19) Kjellander, R.; Marčelja, S. *Chem. Phys. Lett.* **1984**, *112*, 49.
(20) Miklavic, S. J.; Woodward, C. E. *J. Chem. Phys*, in press.
(21) Scheutjens, J. M. H. M.; Fleer, G. J. *Macromolecules* **1985**, *18*, 1882.

Structural Characterization of Model Polyester Polyurethanes Using Time-of-Flight Secondary Ion Mass Spectrometry

Ioannis V. Bletsos and David M. Hercules*

Department of Chemistry, University of Pittsburgh, Pittsburgh, Pennsylvania 15260

Dieter vanLeyen and Alfred Benninghoven

Physikalisches Institut der Universität Münster, D-4400 Münster, FRG

Costas G. Karakatsanis and James N. Rieck

Mobay Corporation, Pittsburgh, Pennsylvania 15205

Received November 7, 1989; Revised Manuscript Received March 9, 1990

ABSTRACT: Time-of-flight secondary ion mass spectra (TOF-SIMS) of a polyester and polyurethanes based on polyesters and diisocyanates were obtained from thin films cast from solution on silver substrates. Intact polyester or polyurethane oligomers and large fragments characteristic of the ester and ester–urethane blocks in polyurethanes, both cationized with Ag^+ and Na^+, were detected in the mass range m/z = 500–3300. The mass of the repeat unit of the polyester in a polyurethane can be determined from the spacing between oligomer or fragment peaks cationized with the same cation. The mass of the urethane can be determined by comparing fragments characteristic of ester and ester–urethane blocks consisting of the same number of repeat units and cationized with the same cation. The combined mass of the terminal groups can be determined from the mass difference between oligomer and fragment ions characteristic of the ester–urethane parts. The masses of unknown alcohol extenders in polyurethanes were determined from m/z values of fragment ions by subtracting the masses of ester and urethane repeat units and cation. The transesterification products of polyester polyurethanes and trifluoroacetic acid were identified from the spectra to be diesters of trifluoroacetic acid and the diol in the polyurethane; they consist of an integral number of ester repeat units with or without a urethane and an additional diol. Differences and similarities between various polyurethanes can be assessed by comparing their fragmentation patterns. Diols and diisocyanates can be identified by comparing fragments with or without a urethane and transesterification products.

Introduction

Polyurethanes (PUR's) are an important class of polymers. Because of the many formulations suitable for a wide variety of applications, PUR's are often difficult to characterize. Hydrolysis, infrared spectroscopy, and nuclear magnetic resonance spectroscopy have been used to determine functional groups in PUR's.[1-4] Pyrolysis mass spectrometry and pyrolysis chromatography mass spectrometry have been used to characterize many PUR's,[5,6] and PUR pyrolytic mechanisms have been proposed.[7] Various spectroscopic techniques used to characterize PUR's and other polymers have been reviewed in detail in previous papers.[8-10] These techniques can provide general information about functional groups in PUR's. More detailed characterization, however, can be difficult and time consuming, and in cases of complicated PUR formulations, standard PUR's must be prepared for comparison purposes. Therefore, the need for more definitive rapid and detailed structural characterization of PUR's still exists.

Successful structural characterization of PUR's includes identification of the repeat unit, its hydroxy and isocyanate components, and chain extenders, their sequence in

0024-9297/90/2223-4157$02.50/0